2.85-Gb/s Organic Light Communication With a 459-MHz Micro-OLED

Mohamed Nihal Munshi, Luc Maret, Benoit Racine, Alexis P. A. Fischer, Mahmoud Chakaroun, and Nixson Loganathan

***Abstract*— We present a broadband free space light communication system using high-speed organic light emitting diodes (OLEDs) as transmitters. Firstly, we report the design and bandwidth measurements of micro-OLEDs with active area of 40 × 40μm^2. For this OLED, a cut-off frequency up to 459 MHz is observed. Secondly, by applying Direct Current Optical Orthogonal Frequency Division Multiplexing (DCO-OFDM) with adaptive bit and energy loading techniques, a data rate of 2.85 Gb/s is achieved. The increase of bandwidth and throughput reported in the current work are attributed to the improvements at the material, device and transmission levels. At the material level, a low work function Calcium cathode and ALD encapsulation of OLED is considered. At the device level, the active area is reduced in size and the OLEDs thickness is optimized. At the transmission level, parameters such as bias voltage, modulation amplitude and clipping have been fine-tuned to obtain high data rate.**

***Index Terms*— Organic light emitting diode, visible light communication, organic optoelectronics, DCO-OFDM.**

I. Introduction

In THE last decade, optical wireless communication, specifically in the realm of visible light communication (VLC), has emerged as a promising technology for connectivity and communication. This is because VLC offers a complementary approach to traditional radio frequency (RF) based wireless communication by operating in the unlicensed optical spectrum. This reduces congestion in the RF spectrum while enabling efficient end-to-end communication. Furthermore, the different light emitters utilized in VLC provide immense potential for improvement at both the device and material levels. Therefore, extensive research has been conducted so far on III-V (inorganic) light emitting diodes (LEDs).

In the last few years, a data rate of 7.7 Gb/s has been reported with a 10-μm-diameter single blue GaN LED exhibiting 200 MHz bandwidth [1]. Another similar study reported the use of a violet micro-LED with diameter of 24 μm, demonstrating a cut-off frequency of up to 655 MHz and a data rate of 7.9 Gb/s [2]. In 2021, L. Wang et al demonstrated even higher bandwidth of up to 1.3 GHz using a blue m-plane epitaxy-based micro-LED with a diameter of 75 μm [3]. Furthermore, the highest throughput of 11 Gb/s was achieved using a 3 × 3 matrix of blue micro-LEDs [4].

Recently, OLEDs have emerged as an alternative due to their inherent advantages, such as lower manufacturing costs, flexibility, and the potential for high speed transmission. Moreover, OLEDs, which were considered as relatively slower devices compared to their inorganic counterparts, have shown noteworthy advancements. In 2007, Barlow and al. reported the potential of a 140-μm diameter green polymer OLED reaching a bandwidth of 16 MHz [5]. More recently, Yoshida et al. conducted a systematic investigation to optimize light emitters and achieved a breakthrough in performance [6]. Using a blue micro-OLED with a diameter of 300 μm, they achieved a data rate of 1.15 Gb/s with a cut-off frequency of 245 MHz. In the meantime, further studies have demonstrated the incorporation of Coplanar Wave-guided (CPW) electrodes for red micro-OLEDs (100-μm diameter), showcasing optical pulses as short as 2.5 ns, thus making them potentially interesting for VLC applications [7], [8]. These aforementioned works indicate that OLEDs can achieve large bandwidths. This potential of organic photonics for light communication was reviewed by Clark et al. in 2010 [9]. Additionally, a recent comprehensive review discussing various aspects of optimizing light emitters for high-speed communication at both the device and material levels is reported in [10]. This review discusses different strategies such as reducing parasitic capacitance and selecting appropriate fluorescent materials.

Our work follows a similar logic and introduces originalities at the material level, device level and transmission level.

At the material level, firstly, emitter with relatively short fluorescence lifetime of 1.7 ns is used. Secondly, the heterostructure is PiN doped to ensure high charge carrier mobility and to reach fast dynamics and short electrical time constant. Thirdly, a low work function Calcium cathode (2.87 eV) is considered to improve electron injection and lower the operating voltage of the OLEDs. Fourthly, the Atomic Layer Deposition unlocks the use of Calcium as low

Manuscript received 1 August 2023; revised 25 September 2023; accepted 15 October 2023. Date of publication 3 November 2023; date of current version 8 November 2023. This work was supported in part by the Agence Nationale de la Recherche (ANR) through the 453 Investissement d'Avenir Programs under Grant ANR-11-IDEX-0005-02; in part by the Labex SEAM: Science Engineering, 454 Advanced Materials; in part by IdEx Université de Paris under Grant ANR-18-IDEX-0001; and in part by ANR funded DEμS CRP Project under Grant ANR-21-CE24-0016-02. *(Corresponding author: Mohamed Nihal Munshi.)*

Mohamed Nihal Munshi is with the Commissariat aux Energies Alternatives et à l'Energie Atomique, 38000 Grenoble, France, and also with Laboratoire de Physique des Lasers, UMR CNRS 7538, and Centrale de Proximité en Nanotechnologies de Paris Nord, Université Sorbonne Paris Nord, 93430 Villetaneuse, France (e-mail: nihal.munshi@cea.fr).

Luc Maret and Benoit Racine are with the Commissariat aux Energies Alternatives et à l'Energie Atomique, 38000 Grenoble, France (e-mail: luc.maret@cea.fr).

Alexis P. A. Fischer, Mahmoud Chakaroun, and Nixson Loganathan are with Laboratoire de Physique des Lasers, UMR CNRS 7538, and Centrale de Proximité en Nanotechnologies de Paris Nord, Université Sorbonne Paris Nord, 93430 Villetaneuse, France (e-mail: fischer@univ-paris13.fr).

Color versions of one or more figures in this letter are available at https://doi.org/10.1109/LPT.2023.3327612.

Digital Object Identifier 10.1109/LPT.2023.3327612

1041-1135 © 2023 IEEE. Personal use is permitted, but republication/redistribution requires IEEE permission.
See https://www.ieee.org/publications/rights/index.html for more information.

Authorized licensed use limited to: CEA GRENOBLE. Downloaded on November 22,2023 at 18:38:21 UTC from IEEE Xplore. Restrictions apply.

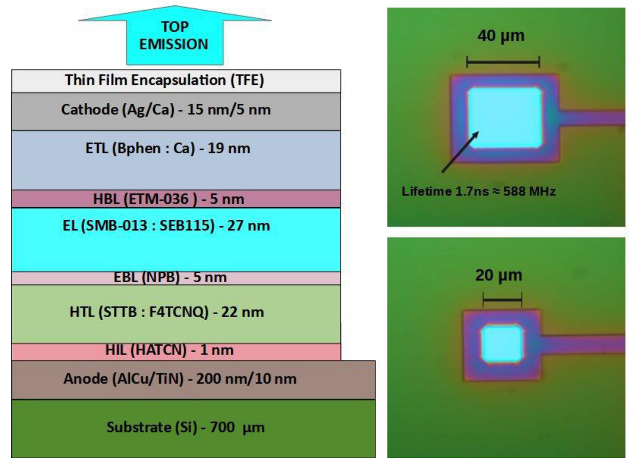

Fig. 1. (Left) PiN OLED heterostructure (Right) Electroluminescent images of 40 × 40µm^2 and 20 × 20µm^2 OLEDs with the shorter fluorescence lifetime of the emitter measured experimentally.

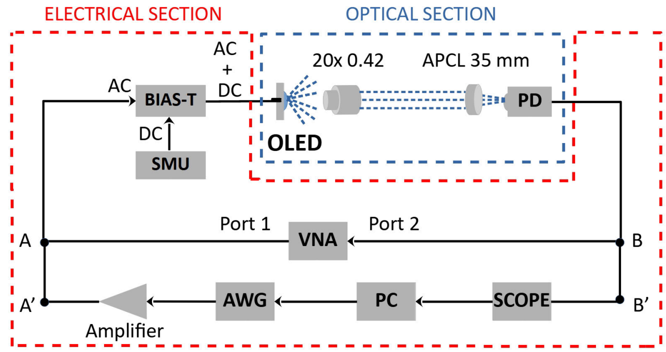

Fig. 2. Experimental setup for bandwidth measurements (VNA) and transmission (Amplifier, AWG, PC, SCOPE).

work function electrode and as a material in PiN doping by providing superior passivation against oxygen and moisture, effectively mitigating the instability resulting from oxidation.

At the device level, firstly, the geometry is reduced in size by a factor of 57 in comparison to previous work in [6]. This reduction in size helps to decrease the parasitic capacitance which in turn reduces the electrical time constant. Secondly, the thickness of the different layers have been optimized to improve charge balance and reduce the overall thickness of the OLEDs, thereby reducing its dynamical resistance. This helps to further reduce the electrical time constant. As a result, large bandwidths while operating at reduced bias voltages are achieved, surpassing previous results.

At the transmission level, DCO-OFDM (Direct Current Optical-Orthogonal Frequency Division Multiplexing) is used to modulate these optimized OLEDs. Moreover, in this technique, the amplitude, clipping, and bias voltage parameters are finely tuned to achieve high data rates.

The letter is structured as follows: Section II describes the design and heterostructure of the OLEDs, followed by Section III where the bandwidth measurements are presented. In Section IV, the transmission and data rates are discussed, and Section V provides some concluding remarks.

II. OLED Design and Heterostructure

In the fabrication process, silicon substrates are used because they offer efficient thermal management and superior heat dissipation compared to glass substrates. This choice was made to ensure optimal performance of the OLEDs. Additionally, the design incorporate OLEDs with small active areas ranging from 40 × 40 µm^2 to 5 × 5 µm^2. Achieving such reduced active areas was made possible through the deposition of organic materials using shadow masks in a thermal vapour chamber (Spectros 150 from Lesker). Furthermore, in the current design, the light-emitting surface area and the electrode pads (Anode and Cathode) were separated by a distance of only 1 mm, resulting in low serial resistance. The aforementioned factor further contributes in reducing the electrical time constant at the device level and improving the bandwidth of the light emitters.

The anode is composed of a layer of Aluminium:Copper (AlCu) and Titanium:Nitrogen (TiN), while the cathode layer consists of Calcium, known for its low work function despite its sensitivity to oxygen. This layer of cathode is covered by a 15 nm layer of Silver. To achieve high luminance from these light emitters, a PiN structure with blue fluorescent emitter was selected, as illustrated in Figure 1. The intrinsic semiconductor region (EL-Emitting Layer), synthesized by livilux®OLED materials of Merck KGaA, Darmstadt, Germany, exhibits a fluorescence lifetime measured at 1.7 ns. It is sandwiched between positive semiconductor region of Hole Injection Layer (HIL)-1,4,5,8,9,11-hexaazatriphenylene-hexacarbonitrile (HATCN), Hole Transport Layer (HTL) -2-(N,N-Dimethylamino)-hexadecafluorohexathiatriphenylene-3-carbonitrile (STTB-F4TCNQ), Electron Blocking Layer (EBL) -N,N'-Bis(1-naphthyl)-N,N'-bis(phenyl) benzidine (NPB) and negative semiconductor region of Electron Injection Layer (EIL) – Calcium (Ca), Electron Transport Layer (ETL) - 4,7 diphenyl-1,10-phenanthroline (Bphen): Calcium (Ca)., Hole Blocking Layer (HBL) – ETM 036. Finally, a capping layer and a protective layer by Atomic Layer Deposition (ALD) process has been added onto the cathode surface to complete the transparent OLED stack and prevent degradation induced by oxygen and humidity. The ALD encapsulation proves crucial to prevent calcium from oxidation, which is key for the OLEDs stability [12].

III. Bandwidth Measurement Of OLED

The micro-OLEDs are then inserted in a transmission chain (as shown in Figure 2) for bandwidth analysis. The transmission chain consists of an electrical section and an optical section. The electrical section consists of a vector network analyzer (VNA Rohde & Schwarz ZNL-14, 5 kHz – 14 GHz) whose port 1 (source port) is connected to a bias-tee (Picosecond 5575A-104, 10 kHz – 12 GHz) that combines the AC signal from VNA with a DC bias from a source meter unit (Keithley 2601A). This biased signal is then fed to the top emitting micro-OLEDs through a radio frequency probe (Picosecond-GSG-100, DC-20 GHz).

The emitted light is collected and collimated onto a photodetector using optical components. Here, the optical section includes an objective, a collimating lens, and an avalanche photodetector (Thorlabs APD210, 5-1000 MHz). To ensure an

Authorized licensed use limited to: CEA GRENOBLE. Downloaded on November 22,2023 at 18:38:21 UTC from IEEE Xplore. Restrictions apply.

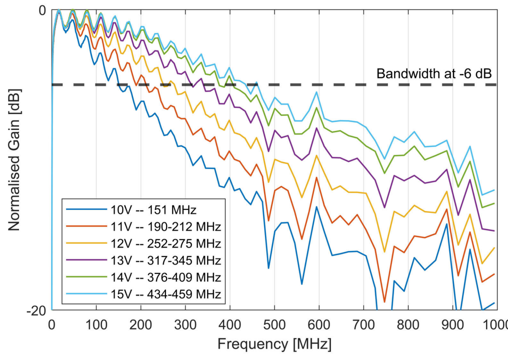

Fig. 3. Bandwidth measurements of 40 μm x 40 μm OLED at different bias voltages.

adequate collection of emitted light while maintaining a long working distance, a Mitutoyo objective with a magnification of 20, a numerical aperture of 0.42, and a focal length of 10 mm is used. This objective with a long working distance of 20.2 mm is chosen to avoid contact with the probe's head due to the short distance of 1 mm between the contact pads for probes and the light-emitting surface area. The collected light from the objective is collimated using an achromatic plano-convex lens with a focal length of 35 mm and directed onto the active area (0.5 mm diameter) of the photodetector. The output of the photodetector is connected to port 2 (receiver port) of the VNA for analysis of the forward transmission coefficient (S21).

In this case, the upper cut-off frequencies of all components in the system including the VNA, coupler, RF probe, APD, and cables, are all above 1 GHz. This implies that any observed overall system cut-off frequency below 1 GHz will be predominantly driven by the OLEDs under operation. However, in our bandwidth estimation, the APD210 photodetector exhibits a lower cut-off frequency starting at 5 MHz. Hence, using a lower frequency photodetector (Thorlabs APD 430A2, DC-400 MHz), a frequency response drop of 1 dB before 5 MHz was measured that is taken into account later in the −6dB bandwidth measurement. The total length of the optical setup, which represents the distance between the optical source and the photodetector, is 250 mm.

The normalised frequency responses of 40 μm OLEDs at different bias voltages are shown in Figure 3. The black dashed line represents −6 dB gain to deduce the cut-off frequency. Here bandwidth increases with the bias voltage. A bias voltage of 15V allows reaching 459 MHz which stands for the highest bandwidth measured for a micro-OLED so far. Also, smaller $20 \times 20\ \mu m^2$ OLEDs were tested, which demonstrated similar results to that of the 40 μm OLEDs. This similarity can be attributed to the fact that both the 40-μm OLED and 20-μm OLED exhibit comparable parasitic capacitance because the total inactive (insulated resin) and active areas remain constant.

IV. Data Rate Measurements

Since the larger OLED emits more light with however similar bandwidth, the transmission is performed using 40-μm OLEDs. For these measurements, the optical part of the setup remains the same as that of bandwidth measurements

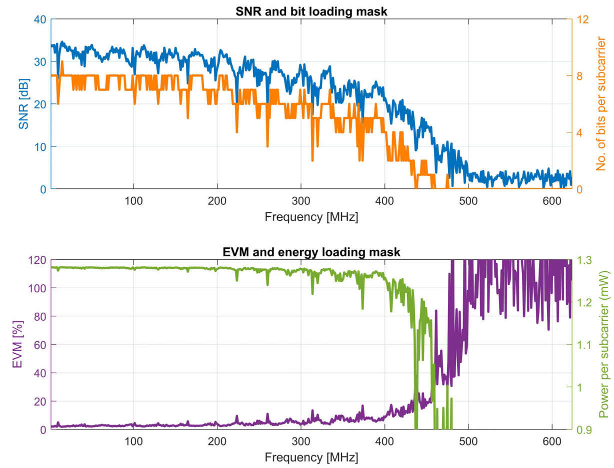

Fig. 4. (Top) SNR and bit loading mask; (Bottom) EVM and energy loading mask of transmission with 40 μm x 40 μm OLED.

(shown in Figure 2): except the photodiode changed for the Thorlabs APD430A2 which shows a relatively higher gain than APD210. Furthermore, even if this avalanche photodiode has a maximum bandwidth of 400MHz lower than the one of the OLED at 15 V_{dc}, it remains relevant since the best data rate performance is reached at $12V_{dc}$, for which the OLED bandwidth is only 275 MHz. Moreover, an optimum bias voltage of 12V is found because if driven at higher voltages, saturation of the OLED luminance degrades the signal to noise ratio (SNR) and therefore the data rate.

In the electrical section, an Arbitrary Waveform Generator (Tektronix AWG5204) with a resolution of 16 bits, a sampling rate of 5 GS/s, and a bandwidth of 2.5 GHz is used for signal generation. For digital signal acquisition, an oscilloscope (Tektronix DPO7254) with a bandwidth of 2.5 GHz and a sampling rate of 40 GS/s is employed. A computer with Matlab© software is used to drive the AWG, oscilloscope, and source meter unit, as well as to perform modulation and receiver post-processing algorithms.

For the modulation scheme, DCO-OFDM is employed due to its spectral efficiency allowing high throughputs [13]. The modulation is based on intensity modulation/direct detection (IM/DD) principle, where the intensity of the light source is modulated by the real OFDM signal. The optical signal is then directly detected using a photodetector. The modulation bandwidth of the system ranges from DC to 625 MHz, and it employs 512 subcarriers. One of the limitation of OFDM is the high peak-to-average power ratio (PAPR) of transmitter's output signal as it restricts the system performance. Hence, clipping of OFDM signal is performed in the time domain at standard deviation of 3.5 to reduce the PAPR and to improve the average power of transmitted output signal. The amplitude of OFDM signal at AWG was set at 400 mVpp, which was then amplified by a wideband amplifier with gain of 25 dB (Mini-Circuits ZHL-72A+, 2.5 kHz - 700 MHz).

The transmitted OFDM signal is then acquired by the scope through the photodetector (APD430A2) and demodulation is performed in software. To maximize throughput, an adaptive bit loading and energy algorithm, as described in [11] is employed. The estimated SNR at the receiver is used to

Authorized licensed use limited to: CEA GRENOBLE. Downloaded on November 22,2023 at 18:38:21 UTC from IEEE Xplore. Restrictions apply.

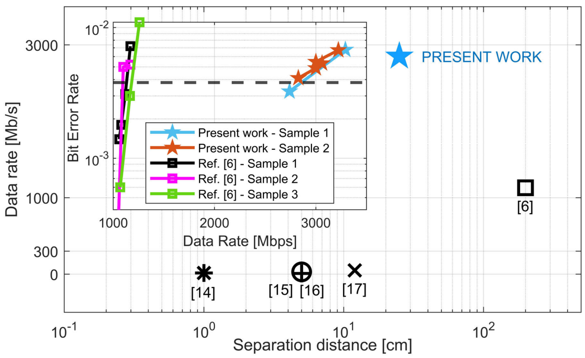

Fig. 5. Measured data rates with respect to transmission distance of present work in comparison to previous works; (Inset) Data rates with respect to different BER of our work and state-of-the-art result (black dashed line – Reference BER of 3.8×10^{-3}).

determine the optimal bit and energy allocation. Figure 4 illustrates the SNR, Error Vector Magnitude (EVM), bit and energy loading mask of the channel as a function of frequency, showing a maximum SNR of approximately 35 dB at lower frequencies. The bit loading mask reveals that 8 bits are transmitted on most of the subcarriers below 200 MHz, while no data is transmitted above 480 MHz leading to high EVM.

In the inset of Figure 5, the measured data rates for different bit error rates (BER) of this work are compared to the state-of-the-art result. From this, a data transmission rate of 2.85 Gb/s corresponding to a reference BER [6] of 3.8×10^{-3} for ensuring reliable communication is noted. Figure 5 compares our data rate as a function of transmission distance to the previous works. It is to note that this throughput is achieved for a shorter communication distance of 25 cm with only 1” optics, compared to the results reached in [6] at 200 cm with larger 2” optics. However, similar levels of light and thus data rates could be expected at higher distance such as 200 cm because the loss of collimated light in free space could be mitigated using appropriate optics.

V. Conclusion

We have reported an OLED with bandwidth up to 459 MHz and a data rate of 2.85 Gb/s. This is achieved by optimization at the material level, device level and transmission level. At the material level, an emitter with short fluorescence lifetime and PiN doping heterostructure is considered for increased mobility, combined with ALD encapsulation for superior moisture resistance. At the device level, the OLED size is reduced by 57-fold to 40×40 μm^2 in comparison to state-of-the-art-work [6] and thickness of organic layers is fine tuned for improved charge recombination. At the transmission level, the different transmission parameters such as amplitude, clipping and bias voltage are optimized for bit and energy loading algorithm. This achieved bandwidth of 459 MHz at 15V represents a 1.8 times improvement compared to the work of 245 MHz at 19V in [6]. Furthermore, it is to note that this factor is obtained at a lower bias voltage of 15V in comparison to 19V in [6]. In addition, the data rate achieved in our work signifies a substantial enhancement of 2.5 times compared to the work in [6]. Our work establishes the highest bandwidth and data rate with an OLED in visible light communication. As a perspective, further bandwidth and data rate enhancement is expected with the integration of coplanar waveguided electrodes in the OLEDs. Furthermore, implementation of digital compensation of nonlinearity could mitigate the OLED saturation effect and allow for higher bias voltage operation and higher AC excursion, resulting in larger data rates.

References

[1] L. Maret, L. N. Dinh, A. Lagrange, P. Demars, L. Dupre, and O. Lartigue, “Reaching 7.7 Gb/s in OWC with DCO-OFDM on a single blue 10-μm GaN micro-LED,” in *Proc. Opt. Wireless Commun. Conf.*, 2020.

[2] M. S. Islim et al., “Towards 10 Gb/s orthogonal frequency division multiplexing-based visible light communication using a GaN violet micro-LED,” *Photon. Res.*, vol. 5, no. 2, p. A35, Apr. 2017, doi: 10.1364/PRJ.5.000A35.

[3] L. Wang et al., “1.3 GHz E-O bandwidth GaN-based micro-LED for multi-gigabit visible light communication,” *Photon. Res.*, vol. 9, no. 5, p. 792, May 2021, doi: 10.1364/PRJ.411863.

[4] E. Xie et al., “Over 10 Gbps VLC for long-distance applications using a GaN-based series-biased micro-LED array,” *IEEE Photon. Technol. Lett.*, vol. 32, no. 9, pp. 499–502, May 1, 2020, doi: 10.1109/LPT.2020.2981827.

[5] I. A. Barlow, T. Kreouzis, and D. G. Lidzey, “A polymer light-emitting diode as an optical communication light source,” *Organic Electron.*, vol. 8, no. 5, pp. 621–624, Oct. 2007, doi: 10.1016/j.orgel.2007.04.003.

[6] K. Yoshida et al., “245 MHz bandwidth organic light-emitting diodes used in a gigabit optical wireless data link,” *Nature Commun.*, vol. 11, no. 1, p. 1171, Mar. 2020, doi: 10.1038/s41467-020-14880-2.

[7] A. C. Chime, S. Bensmida, M. Chakaroun, M. W. Lee, H. Nkwawo, and A. P. A. Fischer, “Electrical modelling and design of ultra-fast micro-OLED with coplanar wave-guided electrodes in ON-OFF regime,” *Organic Electron.*, vol. 56, pp. 284–290, May 2018, doi: 10.1016/j.orgel.2017.12.026.

[8] D. Lenstra, A. P. A. Fischer, A. Ouirimi, A. C. Chime, N. Loganathan, and M. Chakaroun, “Ultra-short optical pulse generation in micro OLEDs and the perspective of lasing,” *J. Opt.*, vol. 24, no. 3, Mar. 2022, Art. no. 034007, doi: 10.1088/2040-8986/ac4cd1.

[9] J. Clark and G. Lanzani, “Organic photonics for communications,” *Nature Photon.*, vol. 4, no. 7, pp. 438–446, Jul. 2010, doi: 10.1038/nphoton.2010.160.

[10] A. Ren et al., “Emerging light-emitting diodes for next-generation data communications,” *Nature Electron.*, vol. 4, no. 8, pp. 559–572, Aug. 2021, doi: 10.1038/s41928-021-00624-7.

[11] A. Leke and J. M. Cioffi, “A maximum rate loading algorithm for discrete multitone modulation systems,” in *Proc. IEEE Global Telecommun. Conf.*, Phoenix, AZ, USA, Nov. 1997, pp. 1514–1518, doi: 10.1109/GLOCOM.1997.644387.

[12] T. Maindron, “Method for encapsulating an organic optoelectronic device,” U.S. Patent WO-0 37 925, Apr. 2010.

[13] S. Dimitrov and H. Haas, *Principles of LED Light Communications: Towards Networked Li-Fi*, 1st ed. Cambridge, U.K.: Cambridge Univ. Press, 2015, doi: 10.1017/CBO9781107278929.

[14] H. Chun, C.-J. Chiang, A. Monkman, and D. O’Brien, “A study of illumination and communication using organic light emitting diodes,” *J. Lightw. Technol.*, vol. 31, no. 22, pp. 3511–3517, Nov. 2013, doi: 10.1109/JLT.2013.2284247.

[15] S. T. Le et al., “10 Mb/s visible light transmission system using a polymer light-emitting diode with orthogonal frequency division multiplexing,” *Opt. Lett.*, vol. 39, no. 13, p. 3876, Jul. 2014, doi: 10.1364/OL.39.003876.

[16] P. A. Haigh et al., “Wavelength-multiplexed polymer LEDs: Towards 55 Mb/s organic visible light communications,” *IEEE J. Sel. Areas Commun.*, vol. 33, no. 9, pp. 1819–1828, Sep. 2015, doi: 10.1109/JSAC.2015.2432491.

[17] H. Chen, Z. Xu, Q. Gao, and S. Li, “A 51.6 Mb/s experimental VLC system using a monochromic organic LED,” *IEEE Photon. J.*, vol. 10, no. 2, pp. 1–12, Apr. 2018, doi: 10.1109/JPHOT.2017.2748152.

Authorized licensed use limited to: CEA GRENOBLE. Downloaded on November 22,2023 at 18:38:21 UTC from IEEE Xplore. Restrictions apply.